LA-UR- 98-3629

Approved for public release; distribution is unlimited.

Title: Neutron Metrology for SBSS

Author(s): C. L. Morris, V. Armijo, J. J. Gomez, G. W. Hart, D. M. Lee, J. D. Zumbro, C. Espinosa, P-25
J. M. Anaya, T. J. Bowles, R. E. Hill, K. B. Morley, S. J. Seestrom, J. Ullmann, P-23
T. N. Taddeucci, W. A. Teasdale, LANSCE-3
S. F. Hahn, NIS-4

Submitted to: DOE OFFICE OF SCIENTIFIC AND TECHNICAL INFORMATION (OSTI)

Los Alamos
NATIONAL LABORATORY

DISCLAIMER

Neutron Metrology for SBSS

C. L. Morris*, J. M. Anaya, V. Armijo, T. J. Bowles, C. Espinosa, J. J. Gomez, S. F. Hahn, G. W. Hart, R. E. Hill, D. M. Lee, K. B. Morley, S. J. Seestrom, T. N. Taddeucci, W. A. Teasdale, J. Ullmann and J. D. Zumbro

Abstract

This is the final report of a two-year, Laboratory Directed Research and Development (LDRD) project at the Los Alamos National Laboratory (LANL). The goal of this work is to develop new detector technologies for Science-Based Stockpile Stewardship (SBSS) at the Los Alamos Neutron Scattering Center (LANSCE) using existing expertise and infrastructure from the nuclear and particle physics programs at LANL.

Background and Research Objectives

Many of the projects envisaged for supporting the Science-Based Stockpile Stewardship (SBSS) program at the Los Alamos Neutron Science Center (LANSCE) require neutron detectors. Currently nearly all of these are limited to what is available commercially. With this project we intend to broaden the range of options available for neutron detectors at LANSCE by leveraging expertise and infrastructure available from the nuclear and particle physics programs at Los Alamos National Laboratory (LANL).

Importance to LANL's Science and Technology Base and National R&D Needs

LANSCE provides many new capabilities for SBSS. Currently the facility and many of he instruments are undergoing a major upgrade. Our overall goal is to improve the detector technology available in the future at LANSCE.

Scientific Approach and Accomplishments

Detectors for High Energy Neutron Radiography

One objective emphasizes an imaging detector for high-energy neutrons for neutron radiography. High-energy neutrons are much better matched to radiographing thick weapons components than x-rays because of the longer mean free paths. Because of this, a given incident flux provides more accurate radiographic information and smaller scatter background. Additionally, the larger cross sections for neutrons on light isotopes lead to more contrast from low-A materials shielded by heavier isotopes in composite objects.

* Principal Investigator, e-mail: cmorris@lanl.gov

One difficulty with using medium-energy neutrons as a radiographic probe is the absence of any suitable imaging detectors. In our initial work we have shown that good position resolution can be obtained using a high-density converter coupled to a position-sensitive detector. Charged particles produced by neutron interactions in the converter are imaged in the detector. Because of the high rates involved, tracking is not possible, so it is important to minimize the thickness of the package to limit the blurring introduced by propagating the charged particles. Initial work concentrated on building one layer of an active readout imaging ion chamber [1]. This detector obtained about 1% detector quantum efficiency and about 1-mm position resolution.

This year we performed experiments at the Weapons Neutron Research (WNR) Facility to demonstrate a new technology using stacked image plates and 1.5-mm thick copper converters. The ion chamber was replaced with an image plate. An image of a drill motor in its case is shown as Figure 1.

A special target was developed for the WNR to reduce the beam spot from approximately 4.5 x 3 cm^2 to a 1-cm-diameter circular spot. A test object, which consisted of a 10-cm-diameter, right circular cylinder of polyethylene inserted into a 15-cm outside diameter, 10-cm inside diameter tube of depleted uranium, was radiographed at several different angular orientations. The radiography magnification was set to be about 1/20, so the expected position resolution was somewhat less than 1 mm. Three holes with diameters of 1.2, 0.6 and 0.3 cm were bored parallel to the axis of the polyethylene.

Some theoretical tomographs of the cylindrical test object were calculated using the standard flux for WNR 4FP30R and neutron total cross sections. Neutrons for energies between 50 and 700 MeV were included in the calculations. A finite Target-4 source size of 1 cm was used, but there was no attempt made to model resolution smearing by nuclear scattering. The calculations are direct geometrical integrations and statistical effects are not included. These results are shown on the left in Figure 2. The image produced from the actual data is displayed on the right. In the tomographic reconstructions shown in Figure 2, all three holes are visible.

Because the holes in the polyethylene represent neutron transmission variations of only 1-3%, they would not be easily visible in a reconstruction of the complete object. To make them visible, the nine views in the sinogram were first averaged and then each individual view was divided by this average prior to linearizing. The resulting reconstructions are shown in Figure 2. More information on these results is available at http://taddeucci.lanl.gov/nrad/tomogrph.htm.

Low-Energy Neutron Detectors

A second objective focuses developing new techniques for detecting neutrons at and below thermal energies. The long-term goal of this effort is to make available new technology for large-area, inexpensive, position-sensitive (wallpaper) detectors. An immediate goal is to provide detectors in support of current LANSCE experiments.

Neutron detection requires a converter in which the neutron produces a charge signal, and a technique to detect the charged signal. At low energies, exothermic neutron absorption reactions such as $^3He(n,p)^3H$ are used. Because of its large cross section and large energy release ^3He is the most commonly employed converter for thermal energy neutrons. In some applications, ^6Li or ^{10}B are employed. At thermal energies and below, the cross sections for these reactions scale as 1/v, where v is the neutron velocity. For ^3He the cross-section, σ, is 500 barns at 1.8 Å. The mean free path, λ, is $1/\rho\sigma = 42$ (cm/bar/$\sqrt{}$ev) and the efficiency, *eff*, is given by: $eff = 1 - e^{-l/\lambda}$.

Scintillators, solid-state detectors and amplifying gas structures have all been employed as detectors. Of these, proportional-chamber detectors are the most common because of ease of construction, ease of operation, and expense. In addition to the ^3He, a higher-density stopping gas is usually needed to limit the range of the charged particle range in order to prevent energy transfer to the detector walls and to limit the size of the interaction so that position-resolution requirements can be met.

We have built a gas handling system, which allowed us to study different gas mixtures and recover the ^3He. We have used this to study various stopping gases. We will extend these studies to determine chamber lifetimes for various stopping gases in the future.

Ultracold Neutron (UCN) Detectors

We have designed and built UCN detectors for FP 11B. These are stable detectors with very good signal-to-noise ratios. The background rates were on the order of 0.02/s. These low backgrounds enabled us to detect UCN at a rate of less than 1/s in our first year of running with the rotor source. We have since improved many aspects of the source and are now up to a production rate of 800/s.

In addition to wall losses, one needs to worry about upscattering of the UCN before they are detected. We have found that the low scattering cross sections for fluorine and carbon make CF_4 an ideal stopping gas for UCN detectors.

A photograph of our UCN detector is shown in Figure 3. The performance of the detector for detecting UNC is shown in Figure 4 where a two-dimensional histogram of

time *vs.* pulse height is shown. The band of uniform pulse heights with no time correlation is due to UCN. The low velocity of the UCN washes out the 50-msec period of the LANSCE spallation source.

Line Readout Detector

Position-sensitive area detectors for neutrons are commercially available. Most of these rely on a capacitive-resistive delay line for encoding the position information. Although this technique is capable of providing good position resolution, ~1% of the delay line length, it is comparatively slow. Typically, several μsec are required to provide an analog position signal. This long time leads to problems at short times (fast neutrons) because of pileup. It is not unusual for this to lead to a several-ms-long dead time at the leading edge of the neutron pulse. We have investigated fast delay line encoding as a solution to this problem. Although this technique has been in use for some time[2] in high-energy nuclear physics, it has not been tried for low-energy neutron detectors.

We completed and tested a 5-cm x 40-cm active-area, fast delay-line-readout, two-dimensional imaging detector for cold neutrons (Figure 5) and used it in the focal plane of the Bragg spectrometer on the ultracold neutron (UCN) rotor on flight path (FP) 11B at LANSCE. The data (Figure 6) from this detector helped us to verify that dynamic distortions of the Bragg reflector were not large enough to influence the UCN production rates. The advantage of this detector over more conventional RC-network-encoding detectors is that it is much faster and essentially immune to dead time caused by the gamma flash.

^{3}He Ion Chamber

We also designed, built, and used a helium-3-filled ion-chamber detector for monitoring neutron fluxes from LANSCE beam lines. We developed a method for obtaining absolute flux measurements by analyzing the fluctuation levels from the detector.

Large Area Detectors

A final objective targets large-area, inexpensive neutron detectors. We have begun development aimed at designing and constructing inexpensive amplifiers and readout electronics for large-area, pad-readout ion-chamber detectors. They should provide a low-cost alternative to the area detectors currently used for neutron work.

The mean free path, λ, for thermal neutron in ^{3}He is about 6 bar-cm. This establishes the minimum cost for an area detector. The cost of the ^{3}He for a two-λ thick

(86% efficient) detector is about \$24000/m^2. High-energy physics has developed the techniques needed for cathode pad readout of multi-wire proportional detectors. It is possible to instrument a pad with a low-noise amplifier and readout for about \$4/channel. For a 1-cm^2 segmented readout, this adds another \$50000/m^2 of cost. It should be possible to produce detectors at a fraction of the cost of current techniques.

Noise levels of several thousand electrons can be achieved for modern pulse amplifiers. Since the charge produced in a neutron interaction in ^{3}He is about 2.5×10^4, no further amplification is needed. This implies that large area ion-chamber structures with segmented readout can provide an inexpensive alternative to multi-wire chambers as low-energy neutron detectors. The absence of wire planes or micro-etched circuit boards for added gain reduces the mechanical complexity of the detectors and allows more flexibility in their mechanical design. For instance, it should be possible to design such a detector to conform to the surface of a sphere.

Design work was begun on a low-cost amplifier and read-out system. This work will continue in the future culminating in beam tests in FY1998-FY1999.

References

1. C, L. Morris *et al.,* "An Integrating Image Detector for High Energy Neutron Radiography," the 5th International Conference on Applications of Nuclear Techniques-Neutrons in Research and Industry, Crete, Greece, June 9-15, (1996).

2. L. G. Atencio, J. F. Amann, R. L. Boudrie, and C. L. Morris, "Delay-Line ReadoutDrift Chambers," *Nucl. Instrum. Methods* **187**, 381 (1981).

Figure 1. Radiograph of a drill motor made with a 1.5-mm-thick copper converter coupled to a single image plate. The neutron source was WNR 4FP30R.

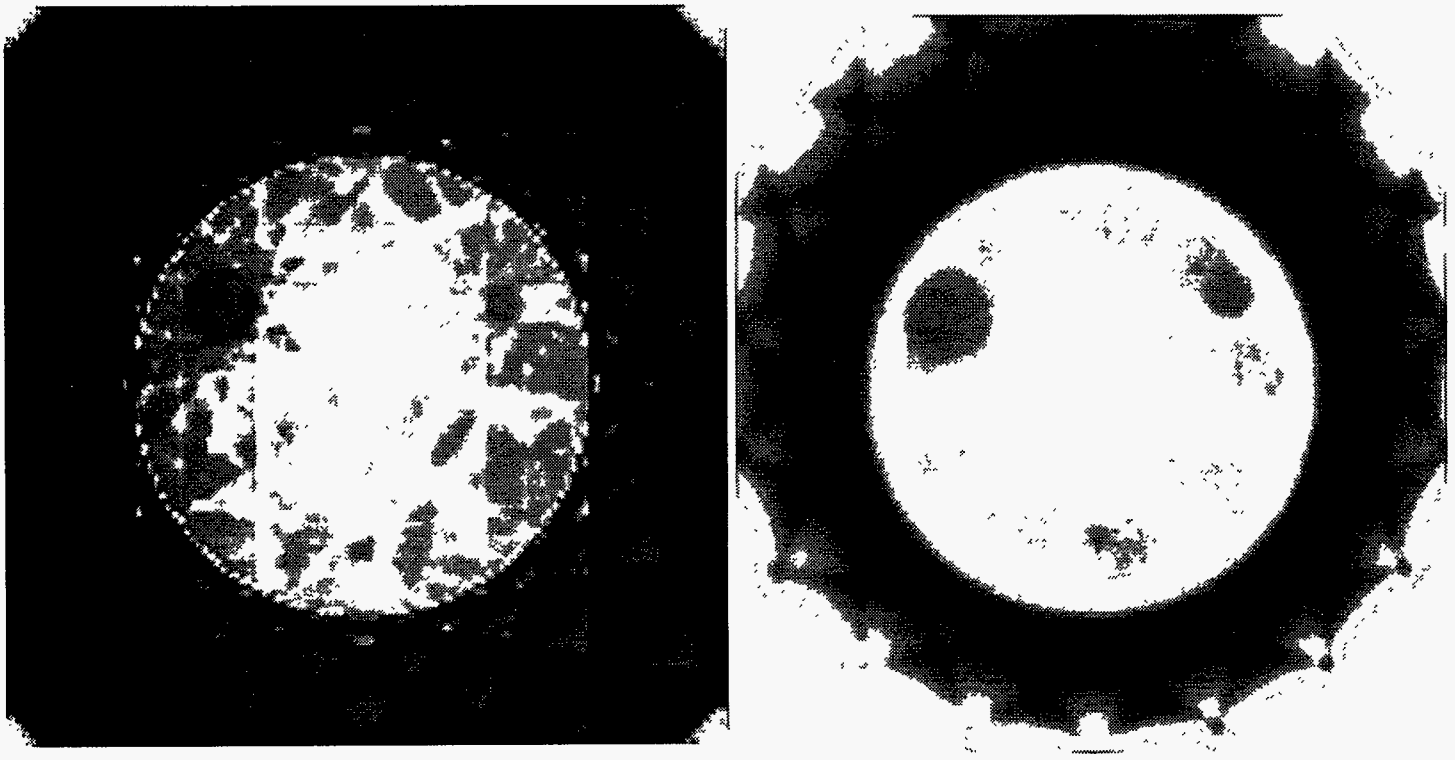

Figure 2. Left: reconstruction from modeled data. Right: reconstruction from the actual data. The pixel size is about 1-mm /pixel. The data outside of the polyethylene insert are not reliable because of the beam size. All three holes in the polyethylene can be observed in both the model and the data.

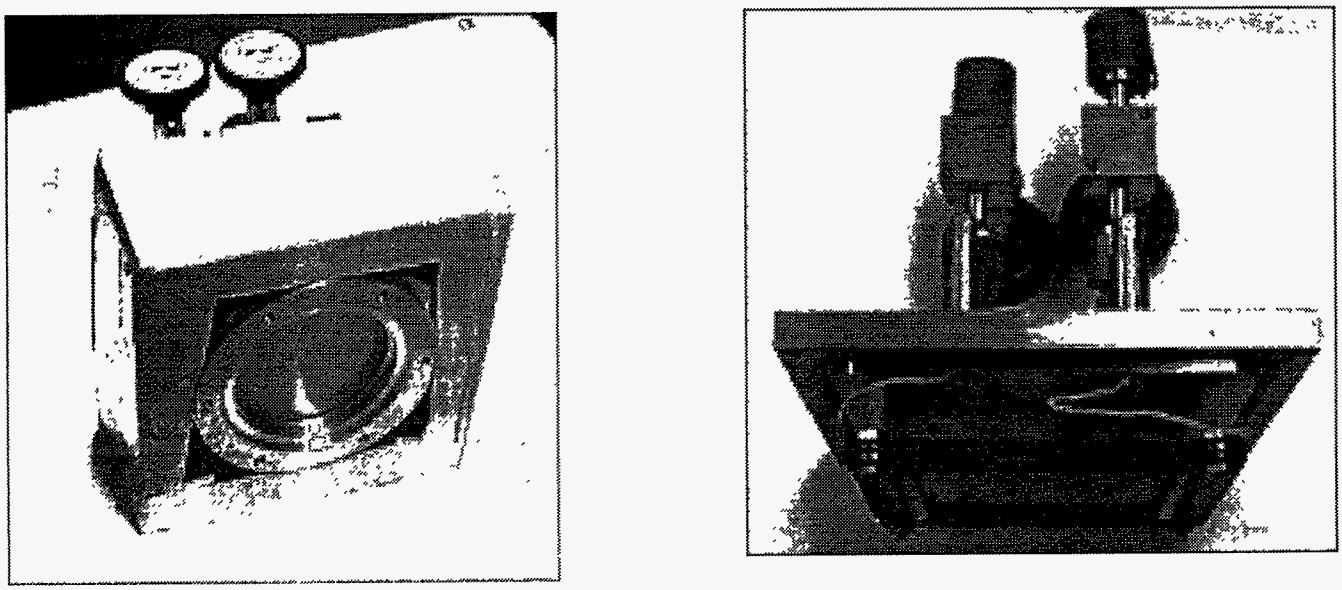

Figure 3. Photographs of the UCN detector.

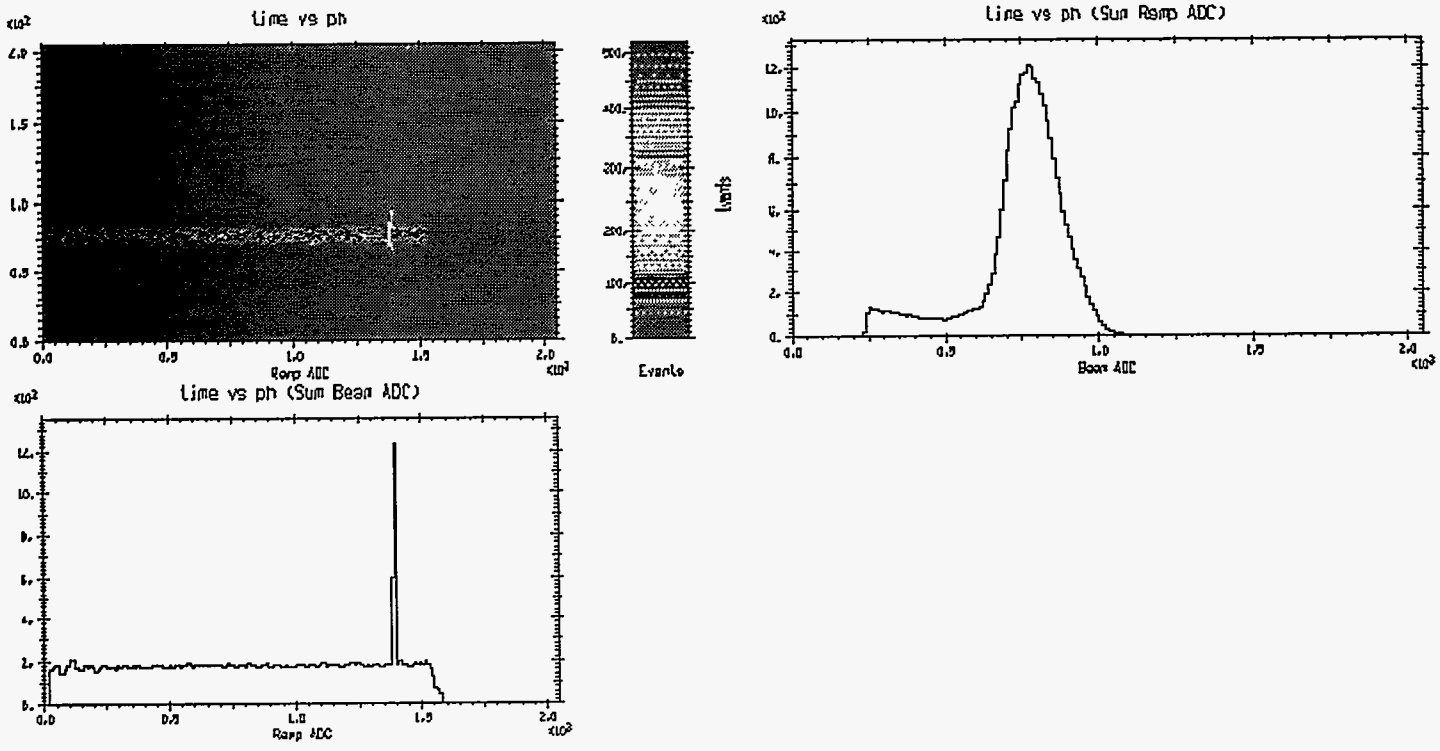

Figure 4. Two-dimensional histogram of time on the horizontal axis and pulse height on the vertical axis.

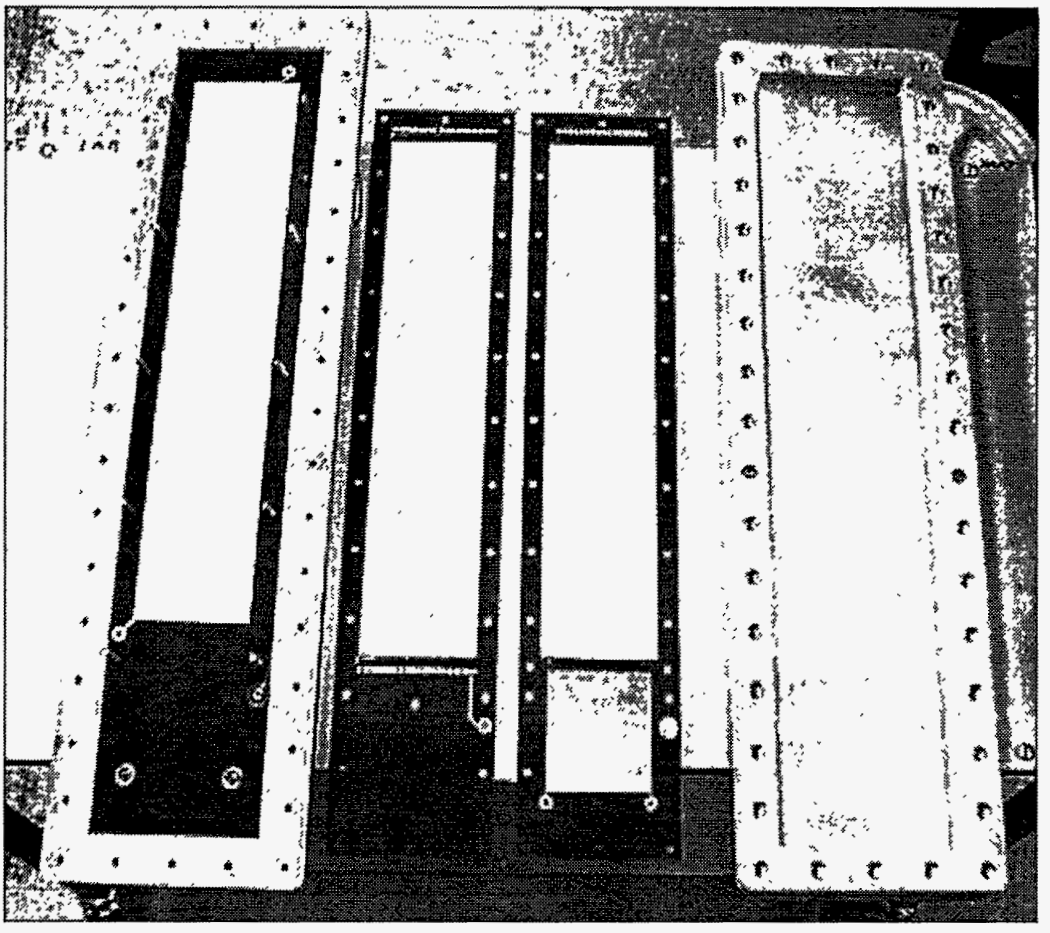

Figure 5. Photographs of the delay-line readout detector.

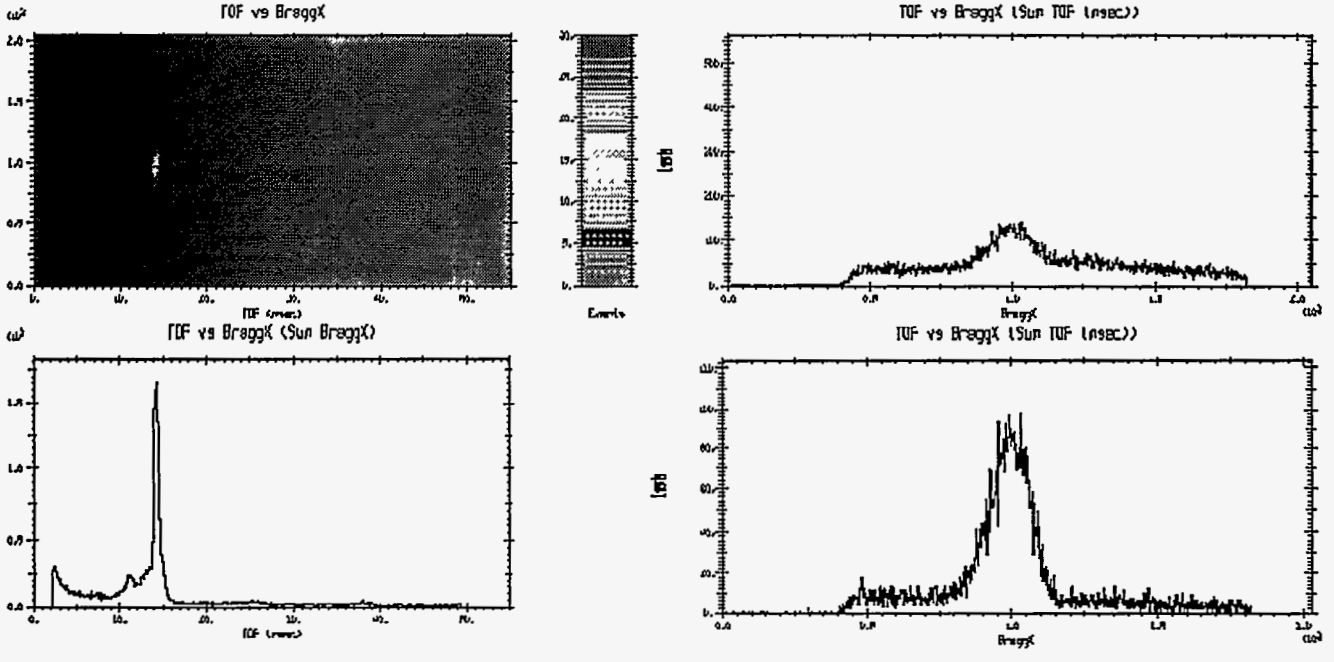

Figure 6. Two-dimensional histogram of Bragg spectrum from the moving rotor.